On the Study of Microstrip Ring and Varactor-Tuned Ring Circuits

KAI CHANG, SENIOR MEMBER, IEEE, SCOTT MARTIN, FUCHEN WANG, AND JAMES L. KLEIN

Abstract — **Equivalent circuits have been derived for microstrip ring and varactor-tuned ring resonators. It was found that the resonant frequency is slightly lower as the coupling gap becomes smaller. Varactor-tuned ring resonators have been developed with up to 15 percent tuning bandwidth using packaged varactor diodes. A dielectrically loaded microstrip ring circuit with lower loss was demonstrated. The results should have many applications in electronically tunable oscillators and filters in both hybrid and monolithic integrated circuits.**

I. Introduction

MICROSTRIP RESONATORS have been widely used for the measurement of dispersion, phase velocity, and effective dielectric constant [1]–[5]. Two types of resonators are generally used: linear resonators and ring resonators. The ring resonator has the advantage of freedom from open-end effects.

Microstrip ring resonators have been studied extensively in the open literature [6]–[11]. Most studies use a field theory approach to investigate the effects of line width, curvature, and dispersion on the resonant frequency. An open-ring resonator with a gap inside the ring was also investigated using a magnetic wall model and perturbation analysis [10], [11]. However, an area that has been neglected is the effect of the coupling gap on the resonant frequency.

The design of the ring dimensions is quite straightforward. A microstrip ring structure resonates if its electrical length is an integral multiple of the guide wavelength. The size of the coupling gap determines the coupling between the microstrip line and the resonator. For better accuracy, it was recognized that excessive loading effects, which would otherwise affect the measurements, should be minimized by loosely coupling the resonator to an external circuit. However, no quantitative analysis of the effects of coupling gaps has been reported in the literature.

To assess the effects of the coupling gap on the resonant frequency, an equivalent circuit for the ring resonator, including the effects of coupling gaps, has been developed. It was found that the resonant frequency decreases slightly as the coupling gap becomes smaller. For most ranges of gap size, the effects on resonant frequency are small and negligible.

Manuscript received April 3, 1987; revised July 13, 1987. This work was supported in part by the Office of Naval Research under Contract N00014-86-K-0348.

The authors are with the Department of Electrical Engineering, Texas A&M University, College Station, TX 77843-3128.

IEEE Log Number 8717123.

The ring can be used as a filter or a stabilization circuit for oscillators. In many applications, it is desirable to have a stable, electronically tunable oscillator. Most frequency-stabilized circuits use dielectric resonators or waveguide cavity circuits which are generally difficult to tune electronically [12]–[16]. This paper reports ring resonator circuits which can be easily fabricated and electronically tuned over a wide frequency range using varactor diodes. Unlike the dielectric resonators, the circuits are amenable to monolithic implementation.

Analysis based upon transmission line theory was developed to model the ring resonator circuits. Three types of varactor-loaded circuits were investigated: a varactor diode mounted inside the ring, two varactor diodes mounted inside the ring, and a varactor diode mounted in the coupling gap. It was found that the ring varactor-loaded circuit gives much wider tuning range than the coupling gap varactor-loaded circuit. The experimental tuning bandwidth agrees fairly well with the theoretical prediction.

Different tuning ranges were obtained with various varactor diodes. Up to 15 percent tuning bandwidth was achieved using M/A COM packaged abrupt junction varactor diodes. It is believed that much wider tuning bandwidth could be achieved by the use of hyperabrupt junction beam-lead varactor diodes.

The coupling loss could be high for a ring resonator with discontinuities and loose coupling. One way to reduce the loss is to overlay the microstrip ring with dielectric layers. Experimental results have shown that the loss can be reduced substantially with a proper covering. A variational method was used to calculate the effects of overlaid layers on the effective dielectric constant and characteristic impedance. The theoretical calculations checked very well with the experimental results. The same techniques can be applied to other components and discontinuities.

II. Effects of Coupling Gap on Microstrip Ring Resonators

A. Equivalent Circuit

If a microstrip line is formed as a closed loop on a substrate as shown in Fig. 1, it resonates at certain frequencies. Without consideration of loading effects, the resonant frequencies can be determined by assuming that the structure will support only waves that have an integral

0018-9480/87/1200-1288$01.00 ©1987 IEEE

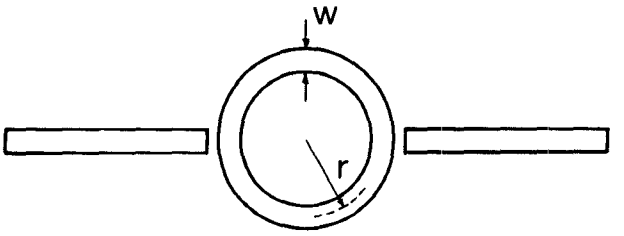

Fig. 1. A ring resonator.

multiple of the wavelength equal to the mean circumference of the ring. This may be expressed as

$$n\lambda_g = 2\pi r \qquad \text{for } n = 1,2,3,\cdots \tag{1}$$

where r is the mean radius of the ring and λ_g is the guide wavelength.

To use the ring for measurement, the ring has to be coupled to an external circuit. This coupling tends to load the ring and thus changes the resonant frequency slightly.

Assuming the two coupling gaps are of the same size, the equivalent circuit of ring resonator is given in Fig. 2. Each half section of ring is represented by a T network with [4, ch. 1]

$$Z_a = jZ_0 \tan\frac{\beta l}{2} \tag{2}$$

$$Z_b = -jZ_0 \csc\beta l \tag{3}$$

where

$$\beta = 2\pi/\lambda_g$$

Z_0 = line characteristic impedance

$$l = \pi r.$$

The coupling gap is modeled by a π-network with C_1 and C_2 found from [17] and [18]. It should be noted that there is an error in the calculation of C_{even} in [17] and [18]. The corrected expression is [19]

$$C_{\text{even}}/w(pF/m) = 12\left(\frac{s}{w}\right)^{m_e}\exp(k_e) \tag{4}$$

where s is the size of the coupling gap and w is the line width.

The definitions for m_e and k_e can be found by [17], [18]

$$m_e = 0.8675 \qquad k_e = 2.043\left(\frac{w}{h}\right)^{0.12} \qquad \text{for } 0.1 \leqslant s/w \leqslant 0.3$$

$$m_e = \frac{1.565}{(w/h)^{0.16}} - 1 \qquad k_e = 1.97 - \frac{0.03}{w/h}$$

$$\text{for } 0.3 \leqslant s/w \leqslant 1.0$$

where h is the thickness of substrate.

For an arbitrary termination of R ohms, the input impedance can be determined by

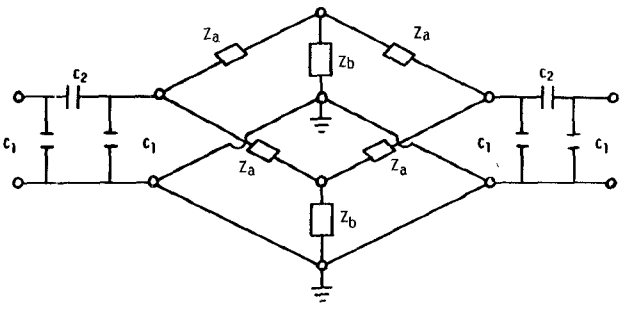

Fig. 2. Equivalent circuit of ring resonator.

where

$$C = \frac{AZ_b^2}{(2A)^2 + (Z_a - 2B - Z_b)^2}$$

$$D = \frac{1}{2}\left[(Z_a - Z_b) - \frac{Z_b^2(Z_a - 2B - Z_b)}{(2A)^2 + (Z_a - 2B - Z_b)^2}\right]$$

and

$$A = \frac{RC_2^2}{(C_1 + C_2)^2 + \left[\omega R\left(C_1^2 + 2C_1C_2\right)\right]^2}$$

$$B = \frac{(C_1 + C_2) + \omega^2R^2\left(C_1^2 + 2C_1C_2\right)(C_1 + C_2)}{\omega(C_1 + C_2)^2 + \omega\left[\omega R\left(C_1^2 + 2C_1C_2\right)\right]^2}.$$

The input impedance is

$$Z_{\text{in}}(\omega) = R_{\text{in}}(\omega) + jX_{\text{in}}(\omega). \tag{7}$$

The resonant frequency can be determined by solving $X_{\text{in}}(\omega) = 0$ or S_{11} = minimum using the bisectional numerical method.

B. Theoretical and Experimental Results

A computer program has been developed to facilitate the calculation. The resonant frequency as a function of gap size is shown in Fig. 3. It can be seen that the resonant frequency is almost constant until the gap becomes very small.

Experiments were carried out to verify the theoretical calculation. The ring was fabricated on Duroid 5870 substrate with 1.62 mm thickness. The experimental results for several gap sizes are also shown in Fig. 3 for comparison.

The unloaded Q for a ring resonator designed at the fundamental resonant frequency of 3.4 GHz is about 180, which agrees with the theoretical results for a typical microstrip line [20]. The loaded Q varies from 20 to 170

$$R_{\text{in}}(\omega) = \frac{C(C_1 + C_2)\left[(C_1 + C_2) - \omega D\left(C_1^2 + 2C_1C_2\right)\right] + \left[D(C_1 + C_2) - \omega^{-1}\right]\left[\omega C\left(C_1^2 + 2C_1C_2\right)\right]}{\left[(C_1 + C_2) - \omega D\left(C_1^2 + 2C_1C_2\right)\right]^2 + \left[\omega C\left(C_1^2 + 2C_1C_2\right)\right]^2} \tag{5}$$

$$X_{\text{in}}(\omega) = \frac{\left[D(C_1 + C_2) - \omega^{-1}\right]\left[(C_1 + C_2) - \omega D\left(C_1^2 + 2C_1C_2\right)\right] - \omega C^2(C_1 + C_2)\left(C_1^2 + 2C_1C_2\right)}{\left[(C_1 + C_2) - \omega D\left(C_1^2 + 2C_1C_2\right)\right]^2 + \left[\omega C\left(C_1^2 + 2C_1C_2\right)\right]^2} \tag{6}$$

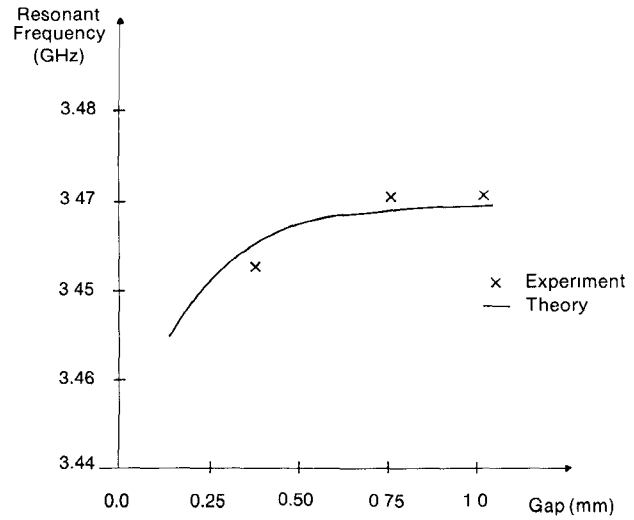

Fig. 3. Resonant frequency as a function of gap dimensions for a ring with $\epsilon_r = 2.33$, $h = 1.62$ mm, $w = 4.72$ mm, and $r = 19.49$ mm.

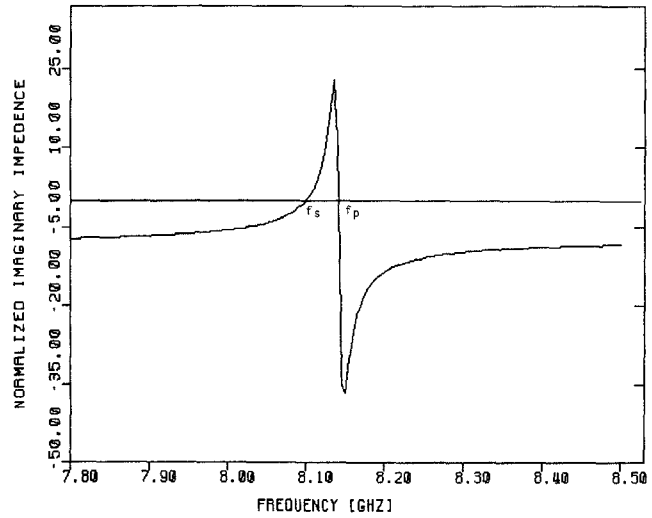

Fig. 5. Input reactance (X_{in}) versus frequency for a typical ring with $\epsilon_r = 10.5$, $h = 0.64$ mm, $w = 0.54$ mm, and $r = 6.49$ mm.

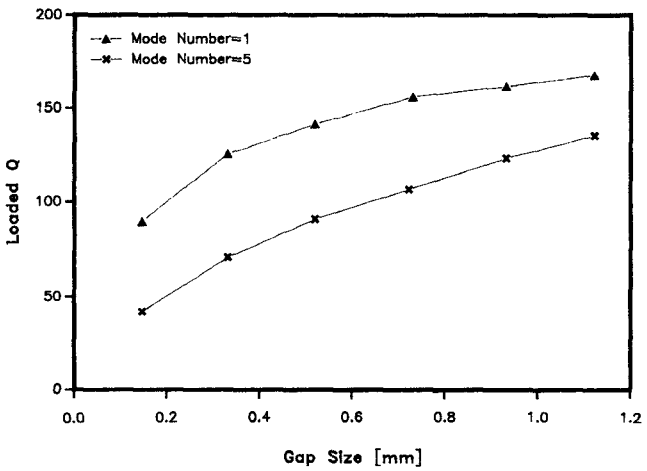

Fig. 4. Loaded Q for a resonant ring as a function of coupling gap size. The parameters used for this experiment are $\epsilon_r = 2.2$, $h = 0.76$ mm, $w = 2.35$ mm, and $r = 10.29$ mm.

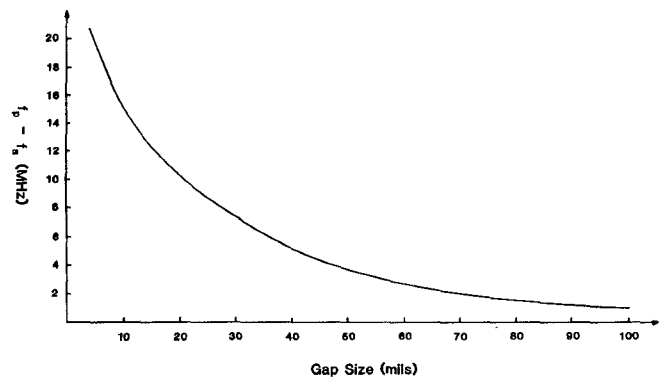

Fig 6. The difference between parallel and series resonance frequency as a function of gap size.

depending on the gap size and the mode number. Fig. 4 shows the measured loaded Q as a function of gap size for $n = 1$ and $n = 5$ modes. It can be seen that the loaded Q is lower for the tight coupling case.

Theoretical results of the input impedance for a typical ring show that the ring resonator has a series resonant frequency (f_s) and a parallel resonant frequency (f_p). An example is given in Fig. 5 for an 8-GHz resonator. The two resonant frequencies are very close to each other. This is reminiscent of a stable piezoelectric crystal oscillator [21] where the circuit will oscillate at a frequency which lies between f_s and f_p but close to the parallel resonance value. The closer f_s and f_p are, the more certain is the resonant frequency. Fig. 6 shows the difference (Δf) between the parallel resonance and series resonance as a function of gap size. It can be seen that for ring resonators with tight coupling (small coupling gaps) the frequency difference Δf is relatively large. As the coupling gap is increased, the series and parallel resonant frequencies approach each other.

III. Varactor-Tuned Ring Resonators

Three types of varactor-loaded circuits were investigated: a varactor diode mounted inside the ring, two varactor diodes mounted inside the ring, and a varactor diode mounted in the coupling gap.

A. Varactor Diode Mounted inside the Ring

The circuit with a varactor diode mounted inside the ring is shown in Fig. 7. Two small gaps were cut in the ring. The gap at the top of the ring is used for varactor mounting. The bottom gap was used for mounting a fixed value dc block capacitor. Bias is supplied through the bias lines. If a big fixed capacitor is mounted in the bottom gap, the equivalent circuit is shown in Fig. 8. As in Fig. 2, the transmission line is represented by a T network and the coupling gaps are modeled by a gap series capacitance (C_2) together with two fringe capacitances (C_1).

Z_ℓ can be modeled by a varactor diode in parallel with a gap capacitance C_2, as shown in Fig. 9. For a packaged diode, the varactor can be represented by a variable junction capacitance $C_j(v)$ in series with a lead inductance L_s. The package capacitance is accounted for by C_p. The

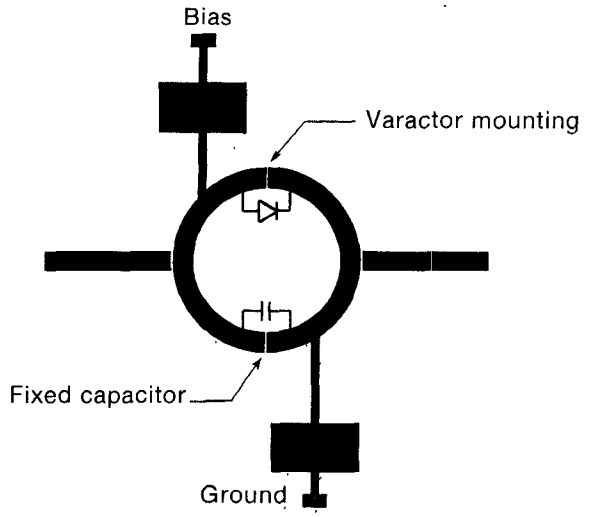

Fig. 7. Varactor-tuned ring resonator circuit with a varactor diode mounted inside the ring.

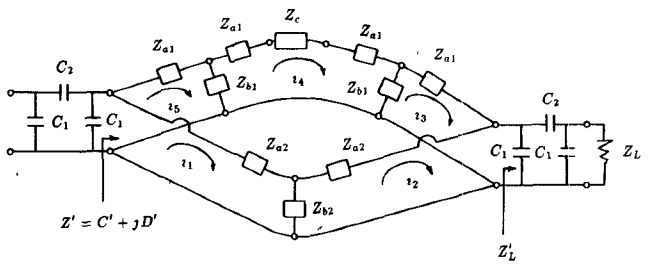

Fig. 8. Equivalent circuit of varactor-tuned ring.

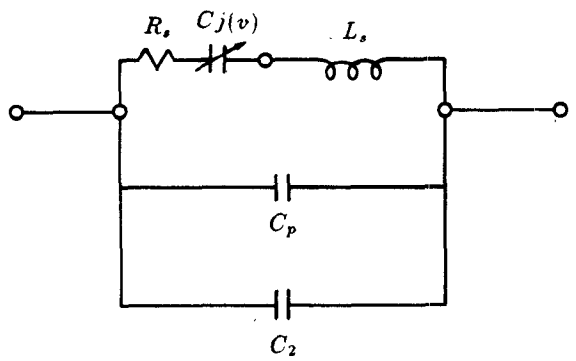

Fig. 9. Equivalent circuit of the varactor diode and mounting gap.

fringe capacitances (C_1) are small and negligible. The series resistance of the varactor is given by R_s.

The input impedance looking into the ring at the gap can be calculated by solving the five loop equations

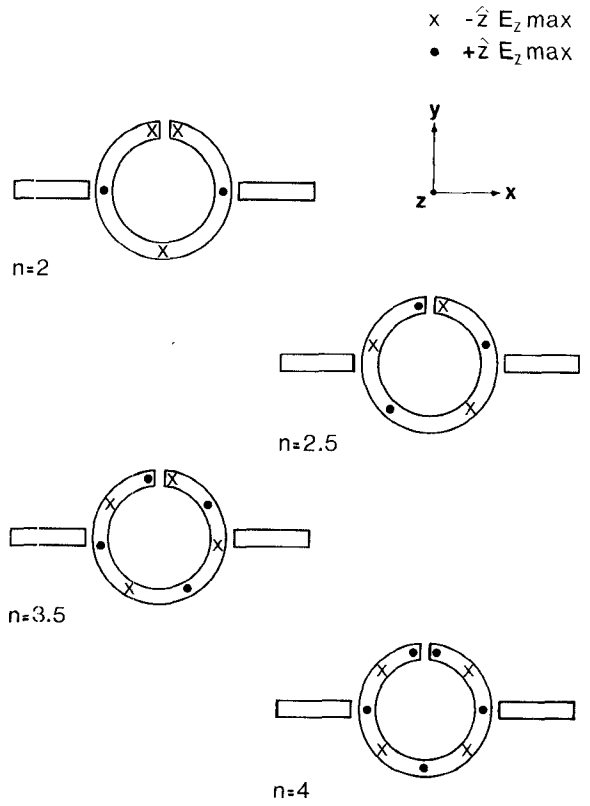

Fig. 10. Mode chart for a ring with a gap.

The input impedance Z_{in} can be found by using (5) and (6) and replacing C and D by C' and D', respectively. The resonant frequency is determined by solving the nonlinear equation for $X_{in}(\omega) = 0$ using the bisectional numerical method. The dispersion effect of microstrip is included in the analysis.

In the measurement of a ring with a gap in the middle of the top half of the ring, it was found that the odd-number modes disappeared. This can be easily explained by examining the boundary conditions imposed on a ring that is broken at a certain point. As shown in Fig. 10, each point that has an open circuit will result in a maximum electric field. For the even modes the break occurs at the electric field maximum and thus the fields are virtually undisturbed. For odd modes the break occurs at what should be an electric field null point; the boundary condition requires the maximum field at the break point and the mode is therefore not present. The break point in the ring also introduces the half-modes which have a positive maximum at one side of the break point and a negative maximum at

$$\begin{pmatrix} Z_{a2}+Z_{b2} & -Z_{b2} & 0 & 0 & 0 \\ -Z_{b2} & Z_{a2}+Z_{b2}+Z'_L & Z'_L & 0 & 0 \\ 0 & Z'_L & Z_{a1}+Z_{b1}+Z'_L & -Z_{b1} & 0 \\ 0 & 0 & -Z_{b1} & 2Z_{a1}+2Z_{b1}+Z_c & -Z_{b1} \\ 0 & 0 & 0 & -Z_{b1} & Z_{a1}+Z_{b1} \end{pmatrix} \cdot \begin{pmatrix} i_1 \\ i_2 \\ i_3 \\ i_4 \\ i_5 \end{pmatrix} = \begin{pmatrix} V \\ 0 \\ 0 \\ 0 \\ V \end{pmatrix} \tag{8}$$

$$Z' = C' + jD' = \frac{V}{i_1 + i_5}. \tag{9}$$

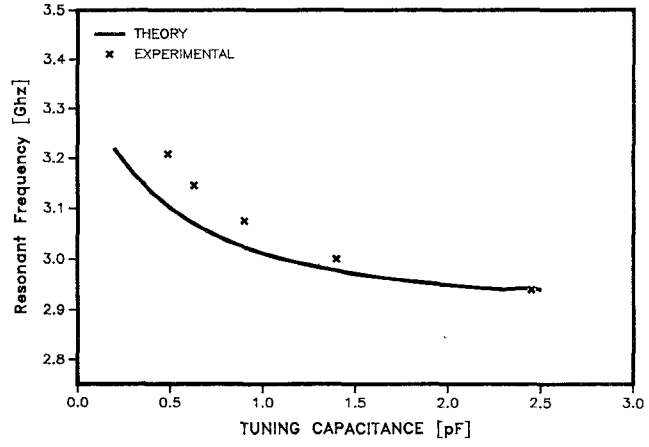

Fig. 11 Resonant frequency of a varactor-tuned ring as a function of varactor tuning capacitance for a circuit with one varactor diode mounted inside the ring.

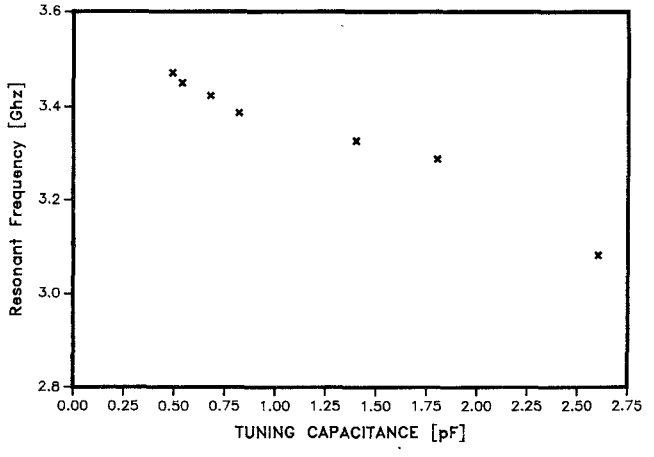

Fig. 12. Measured resonant frequency of a varactor-tuned ring as a function of varactor tuning capacitance for a circuit with two varactor diodes mounted inside the ring.

the other side. It is these modes that will be effectively tuned by the varactor.

A resonant ring was fabricated on Duroid 6010 substrate with 0.635-mm thickness. The theoretical and experimental tuning curves as a function of tuning capacitance are shown in Fig. 11. The resonant frequency was tuned from 2.9 to 3.2 GHz. The varactor used here is from M/A COM (Model 46600) with a capacitance varied from 0.5 to 2.5 pF. It is believed that a much wider tuning range can be achieved if a hyperabrupt junction varactor diode is used. The experimental tuning bandwidth agrees very well with the theoretical prediction from the circuit model. The discrepancies are mainly due to the estimate in the package parasitics.

B. Two Varactor Diodes Mounted inside the Ring

The bottom gap shown in Fig. 7 can be used to mount another varactor diode instead of a fixed-value capacitor. In this case, we have two varactor diodes mounted inside the ring and the tuning range can be substantially increased. Fig. 12 shows the experimental results obtained by using the ring described in subsection A. The tuning

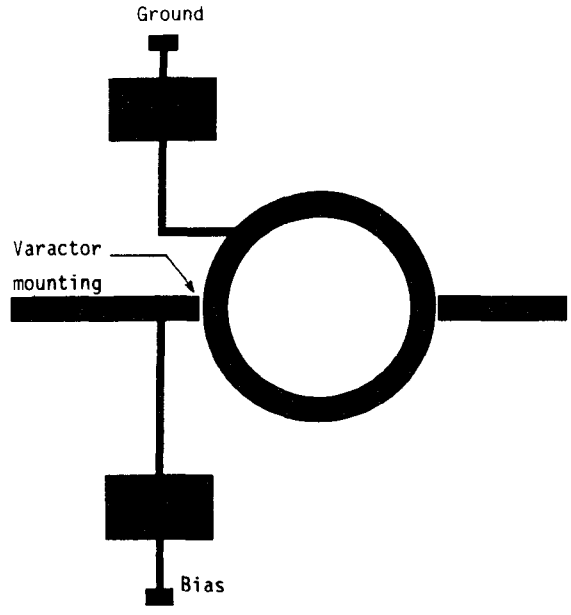

Fig. 13. A varactor diode mounted across the coupling gap.

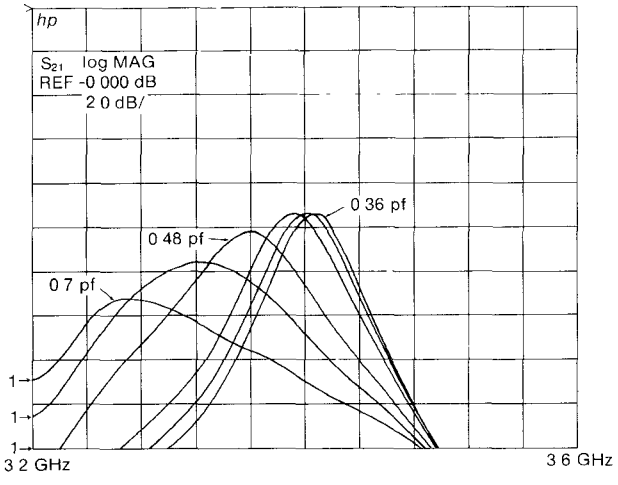

Fig. 14. Resonant frequency of a varactor-tuned ring as a function of varactor capacitance for a circuit with a varactor mounted across the coupling gap

bandwidth is about 15 percent. Theoretical results can be obtained by modifying the equivalent circuit given by Fig. 8.

C. A Varactor Diode Mounted across the Coupling Gap

A coupling gap varactor-loaded circuit, shown in Fig. 13, was also fabricated and tested. The resonant frequency varies with the varactor capacitance, as shown in Fig. 14. It can be seen that the resonant frequency and loaded Q decrease as the varactor capacitance increases. Since a big varactor capacitance corresponds to a small coupling gap, these results agrees with the gap effects on resonant frequency and loaded Q described in Section II. This circuit only works for a small value of capacitance since a large capacitance will bridge the coupling gap and the ring will no longer behave as a resonator. The circuit has limited applications due to its narrow tuning bandwidth.

IV. Dielectrically Loaded Microstrip Circuits

To reduce the coupling loss of the ring resonator, a dielectrically loaded (or dielectrically shielded) microstrip circuit was investigated. The overlaid dielectric layer increases the electric field coupling across the gap, resulting in a larger coupling capacitance. This is equivalent to a smaller effective coupling gap. The covering also reduces the radiation loss. Rings were built using the characteristic impedance and guide wavelength calculated based on a theoretical analysis.

The dielectrically loaded circuit is shown in Fig. 15. A microstrip line with a width w, a dielectric constant ϵ_1, and a substrate thickness h_1 is covered by another dielectric layer of thickness h_2 and dielectric constant of ϵ_2. For low loss, ϵ_2 is chosen to be greater than ϵ_1. Both coupling loss and radiation loss are substantially reduced by the covering.

Analyses of a microstrip covered by a dielectric layer have been reported in the literature [22]–[24]. A variational method based on Green's function was used to solve the line capacitance as associated with this geometry for its simplicity [22]. By assuming a trial function of charge distribution along the line, we can solve the line capacitance C as given below:

$$C = \frac{(1+0.25A)^2}{\sum_{n=\text{odd}} (T_n P_n / Y)} \tag{10}$$

where

$$T_n = (L_n + AM_n)^2$$

$$L_n = \sin(\beta_n w/2)$$

$$M_n = \left(\frac{2}{\beta_n w}\right)^3 \left\{3\left[\left(\frac{\beta_n w}{2}\right)^2 - 2\right]\cos\left(\frac{\beta_n w}{2}\right) + \left(\frac{\beta_n w}{2}\right) \cdot \left[\left(\frac{\beta_n w}{w}\right)^2 - 6\right]\sin\left(\frac{\beta_n w}{2}\right) + 6\right\}$$

$$P_n = \frac{2}{n\pi}\left(\frac{2}{\beta_n w}\right)^2$$

$$A = -\frac{\sum_{n=\text{odd}} (L_n - 4M_n) L_n P_n / Y}{\sum_{n=\text{odd}} (L_n - 4M_n) M_n P_n / Y}.$$

Y is the admittance seen by the strip at the conductor plane. The effective dielectric constant can be found from

$$\epsilon_{\text{eff}} = \frac{C}{C_a} \tag{11}$$

with C_a the line capacitance when the dielectric substrates are absent. The characteristic impedance of the line can be found by

$$Z_0 = \frac{1}{c\sqrt{CC_a}} \tag{12}$$

where c is the speed of light.

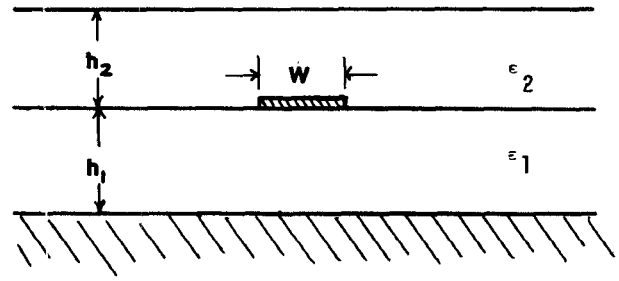

Fig. 15. Dielectrically loaded microstrip line.

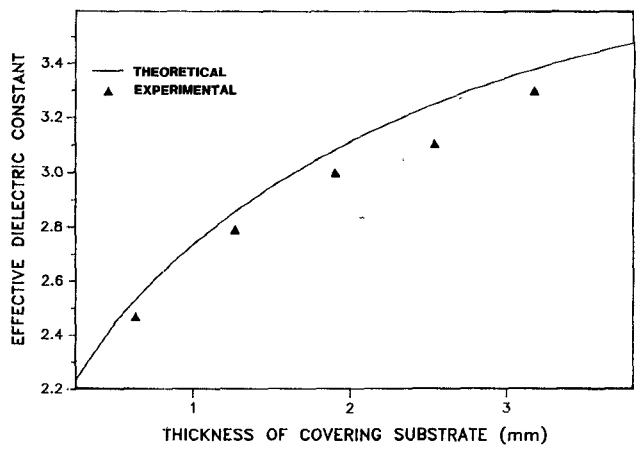

Fig. 16. Effective dielectric constant as a function of thickness for covering substrate with a dielectric constant of 10.5.

Ring resonators have been fabricated to confirm the theoretical results. From the measurement of the resonant frequency, one can calculate the effective dielectric constant by the following equation:

$$\epsilon_{\text{eff}} = \left(\frac{nc}{2\pi r f_r}\right)^2 \tag{13}$$

where r is the mean radius of the ring, f_r is the resonant frequency, and n is the number of operating mode.

Fig. 16 shows the comparison of the calculated effective dielectric constant with the experimental results for different covering dielectric thickness. The covering substrate has a dielectric constant of 10.5. The microstrip used for the experiment has a substrate thickness of 1.57 mm and a dielectric constant of 2.33. It can be seen that the effective dielectric constant increases with the covering substrate thickness. The theory agrees quite well with the experimental data. The slight difference is believed due to the small air gap that exists between the microstrip and the covering layer.

The ring resonator generally has a high insertion loss due to the discontinuities and loose coupling between the ring and lines. By utilizing a dielectric overlaid layer, the coupling can be enhanced and the loss can be substantially reduced.

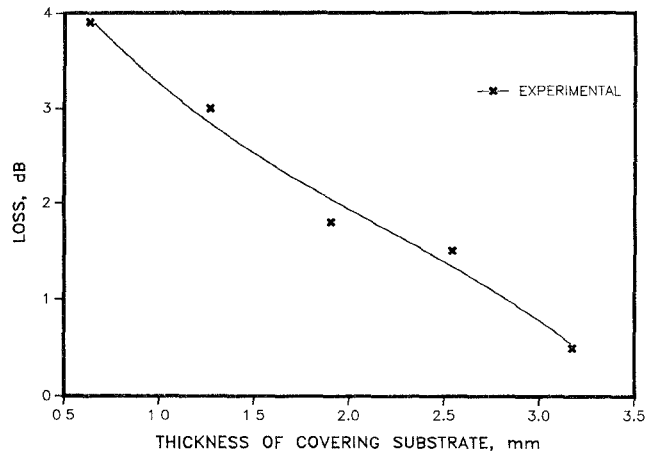

Fig. 17. Insertion loss measurement as a function of covering substrate thickness.

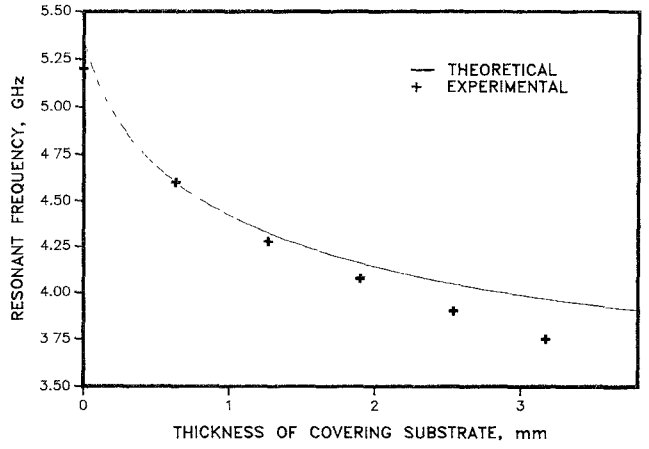

Fig. 18. Resonant frequency as a function of covering substrate thickness. The ring was designed at 5.3 GHz and covered by a substrate with a dielectric constant of 10.5.

Fig. 17 shows the effects of the dielectric covering layer. The total loss of the ring can be reduced to less than 1 dB by using a thick dielectric layer. The covering material has a dielectric constant of 10.5. The rings were designed based upon the calculated effective dielectric constant using (10) and (11). It can be seen that the dielectric layer effectively increases the coupling and reduces the insertion loss.

The covering layer changes the guide wavelength and resonant frequency. The resonant frequency can be determined by the calculated effective dielectric constant. Fig. 18 shows both the calculated and the measured results for a ring covered with different dielectric thicknesses. The resonant frequency drops substantially with the increase of covering thickness. Since the dielectric covering increases the coupling, which is equivalent to a smaller effective coupling gap, the loaded Q decreases as the covering thickness is increased.

V. Conclusions

Equivalent circuits have been derived for microstrip ring and varactor-tuned ring resonators. It was found that the resonant frequency is slightly lower as the coupling gap becomes smaller. The effects are small and generally negligible unless a very small coupling gap is used. Varactor-tuned ring resonators were developed with a tuning bandwidth of up to 15 percent of the operating frequency. A dielectrically loaded technique was demonstrated in reducing the insertion loss of the resonant ring to less than 1 dB. The results presented should have many applications in microwave measurements, electronically tunable filters, and varactor-tuned oscillators.

Acknowledgment

The authors would like to thank Dr. H. Taylor and Dr. M. Weichold for many helpful suggestions and discussions.

References

[1] P Troughton, "High Q-factor resonator in microstrip," *Electron. Lett.*, vol. 4, pp. 520–522, 1968.
[2] P. Troughton, "Measurement techniques in microstrip," *Electron Lett.*, vol. 5, pp. 25–26, 1969.
[3] T C. Edwards, "Microstrip measurements," in *IEEE MTT-S Int. Microwave Symp. Dig.*, 1982, pp 338–341.
[4] T. C. Edwards, *Foundations for Microstrip Circuit Design*. New York: Wiley, 1981.
[5] H. J. Finlay *et al.* "Accurate characterization and modeling of transmission lines for GaAs MMIC's," *IEEE MTT-S Int. Microwave Symp. Dig.*, 1986, pp. 267–270.
[6] I Wolff and N. Knoppik, "Microstrip ring resonator and dispersion measurement on microstrip lines," *Electron. Lett.*, vol 7, pp. 779–781, Dec 30, 1971.
[7] Y S. Wu and F. J Rosenbaum," "Mode chart for microstrip ring resonators," *IEEE Trans. Microwave Theory Tech.*, vol MTT-21, pp 487–489, July 1973.
[8] R. P Owens, "Curvature effect in microstrip ring resonators," *Electron. Lett*, vol 12, pp. 356–357, July 8, 1976.
[9] S. G. Pintzos and R Pregla, "A simple method for computing the resonant frequencies of microstrip ring resonators," *IEEE Trans. Microwave Theory Tech.*, vol. MTT-26, pp. 809–813, Oct 1978.
[10] I. Wolff and V. K. Tripathi, "The microstrip open-ring resonator," *IEEE Trans. Microwave Theory Tech.*, vol MTT-32, pp. 102–106, Jan 1984
[11] V. K. Tripathi and I Wolff, "Perturbation analysis and design equations for open- and closed-ring microstrip resonators," *IEEE Trans. Microwave Theory Tech*, vol. MTT-32, pp. 405–409, Apr 1984
[12] J K. Plourde and C. L. Ren, "Application of dielectric resonators in microwave components," *IEEE Trans. Microwave Theory Tech*, vol MTT-29, pp 754–770, Aug. 1981.
[13] M. Dydyk, "Apply high-Q resonators to mm-wave microstrip,' *Microwaves*, pp 62–63, Dec. 1980.
[14] M Stiglitz, "Dielectric resonators: Past, present, and future," *Microwave J.*, pp 19–36, July 1981.
[15] A Grote, R S. Tahim, and K. Chang, "Miniature millimeter-wave integrated circuit wideband downconverter," in *1985 IEEE MTT Microwave Symp. Dig*, June 1985, pp. 159–162.
[16] K K Agarwal, "Dielectric resonator using GaAs/GaAlAs heterojunction bipolar transistors," in *1986 IEEE MTT Microwave Symp Dig*, June 1986, pp. 95–98.
[17] K. C Gupta, R Garg, and I. J Bahl, *Microstrip Lines and Slotlines*. Dedham, MA: Artech House, 1979.
[18] R Garg and I J. Bahl, "Microstrip discontinuities," *Int J. Electron.*, vol 45, pp 81–87, July 1978.
[19] I. J Bahl, private communication.
[20] A. Gopinath, "Maximum Q-factor of microstrip resonators," *IEEE Trans. Microwave Theory Tech.*, vol MTT-29, pp. 128–131, Feb 1981
[21] J. Millman and C. C Halkias, *Electronic Devices and Circuits*. New York. McGraw-Hill, 1967, pp 535–537.
[22] B. Bhat and S K. Koul, "Unified approach to solve a class of strip and microstrip-like transmission lines," *IEEE Trans. Microwave Theory Tech*, vol. MTT-30, pp. 679–686, May 1982.
[23] I. J Bahl and S. S. Stuchly, "Analysis of a microstrip covered with a lossy dielectric," *IEEE Trans Microwave Theory Tech.*, vol MTT-28, pp. 104–109, Feb. 1980.

[24] V. K. Tripathi and R. J. Bucolo, "A simple network analog approach for the quasi-static characteristics of general lossy, anisotropic, layered structures," *IEEE Trans. Microwave Theory Tech.*, vol. MTT-33, pp. 1458–1464, Dec. 1985.

✠

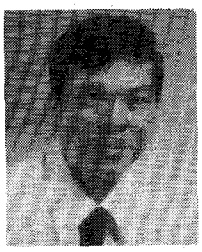

Kai Chang (S'75–M'76–SM'85) received the B.S.E.E. degree from National Taiwan University, Taipei, Taiwan, the M.S. degree from the State University of New York at Stony Brook, and the Ph.D. degree from the University of Michigan, Ann Arbor, in 1970, 1972, and 1976, respectively.

From 1972 to 1976 he worked for the Microwave Solid-State Circuits Group, Cooley Electronics Laboratory, University of Michigan, as a research assistant. From 1976 to 1978 he was employed by Shared Applications, Ann Arbor, where he worked in computer simulation of microwave circuits and microwave tubes. From 1978 to 1981, he worked for the Electron Dynamic Division, Hughes Aircraft Company, Torrance, CA, where he was involved in the research and development of millimeter-wave-devices and circuits. This activity resulted in state-of-the-art IMPATT oscillator and power combiner performance at 94, 140, and 217 GHz. Other activities included silicon and gallium arsenide IMPATT diode design and computer simulation, Gunn oscillator development, and monopulse comparator and phase shifter development. From 1981 to 1985 he worked for TRW Electronics and Defense, Redondo Beach, CA, as a section head in the Millimeter-Wave Technology Department, developing state-of-the-art millimeter-wave integrated circuits and subsystems including mixers, Gunn VCO's, IMPATT transmitters and amplifiers, modulators, upconverters, switches, multipliers, receivers, and transceivers. In August 1985, he joined the Electrical Engineering Department of Texas A&M University as an Associate Professor. His current interests are in microwave and millimeter-wave devices and circuits, microwave–optic interactions, and radar systems.

Dr. Chang is the editor of the *Handbook of Microwave and Optical Components*, to be published by Wiley & Sons, Inc. He has published over 70 technical papers in the areas of microwave and millimeter-wave devices and circuits.

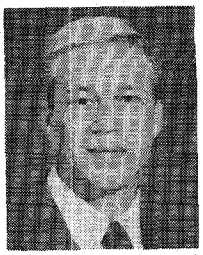

Scott Martin was born in Levelland, TX, on March 6, 1964. In 1986 he received the B.S. degree in electrical engineering from Texas A&M University, where he is currently working towards the M.S. degree. Mr. Martin is a member of Eta Kappa Nu. He received the 1987 IEEE Microwave Fellowship.

✠

Fuchen Wang was born in Jilin, China, on February 18, 1936. He graduated from Qinghua University, Beijing, in 1963. From 1963 to 1968 he was with the Hebei Semiconductor Research Institute, China, where he was engaged in the design, fabrication, and testing of microwave mixer diodes. In 1968 he joined the Nanjing Solid-State Devices Research Institute. From 1968 to 1979 he was a Group Head, working in the area of microwave and millimeter-wave Gunn and IMPATT oscillators. From 1979 to 1985 he was a Vice-Director of a laboratory working on development of GaAs microwave monolithic integrated circuits. Since 1985 he has been an Engineering Research Associate in the Department of Electrical Engineering, Texas A&M University, involved in research on microwave integrated circuits.

✠

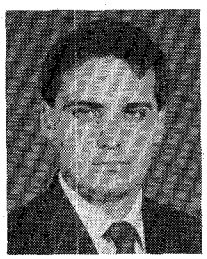

James L. Klein was born in Devine, TX, on August 29, 1964. He received the B.S. degree in electrical engineering from Texas A&M University in 1986. Since June 1986 he has been employed as a Research Assistant in the Microwave–Microelectronics Laboratory at Texas A&M University and is currently working toward the M.S. degree.